Certification of null correctors for primary mirrors

Jim Burge
Steward Observatory Mirror Laboratory, University of Arizona
Tucson, Arizona 85721

ABSTRACT

An optical test for measuring null correctors has been developed that uses a rotationally symmetric computer-generated hologram (CGH) to synthesize the wavefront that would be reflected by a perfect primary mirror. The test of a null lens is performed by measuring the CGH through the null corrector. Agreement between the null lens and the CGH indicates a high probability that both the null lens and the CGH are correct. This paper presents results that confirm the ease and accuracy of the test. Three null correctors for 3.5-m primary mirrors were measured at the Steward Observatory Mirror Lab using this test. Two of the null correctors were shown to have the correct conic constants within the measurement uncertainty of ±78 ppm. The test of the third null corrector was limited by gross flaws in the holograms caused by a fabrication error. A proposed solution to the fabrication problem is presented.

1. INTRODUCTION

Large primary mirrors for optical telescopes are usually interferometrically tested using null correctors. In fabricating a primary mirror, the optical surface is polished to precisely match the wavefront generated by the null corrector. In the unlikely event of a flawed null corrector, the final shape of the primary mirror will be incorrect. Two recent telescopes had their primary mirrors made to the wrong shape because of errors in the null correctors -- the Hubble Space Telescope[1] and the European New Technology Telescope[2]. If accurate testing of the null correctors had been performed, the errors would have been discovered and corrected in the shop. Instead, the errors were not discovered until the finished mirrors were operational in their telescopes.

This paper describes the CGH null lens test and gives results from the measurement of several null correctors. More thorough analysis of the test design and sources of error are given elsewhere[3,4]. Two null correctors for 3.5-m primary mirrors were successfully measured to an accuracy of ±78 ppm in the conic constant. Unexpected hologram fabrication errors limited the test of a third null corrector. Plans for circumventing the fabrication error and for testing a null corrector for a 6.5-m $f/1.25$ primary are discussed.

The holographic test of null correctors fills an important gap in the fabrication of highly aspheric optics. Because the null correctors for steep aspheres introduce hundreds of waves of asphericity, they are complex and sensitive to manufacturing errors. A small manufacturing flaw or oversight may cause significant aberration in the null lens resulting in a mirror finished to the wrong shape. Therefore, the verification of the test optics is viewed as a critical step in the fabrication of highly aspheric optics. One method for verifying the optical test is to compare results from two independent null lenses. This can be expensive and inconclusive. (What if the two null lenses do *not* agree?) Another technique is to perform an independent test on the completed mirror such as a scanning pentaprism test[3,5,6]. Accurate tests of this type are difficult and expensive, and if an error is detected in the finished mirror, it is too late. Either the mirror or the telescope must be corrected.

0-8194-1243-0/94/$6.00

1.1. DESCRIPTION OF HOLOGRAPHIC NULL LENS TEST

In the CGH null lens test, a computer-generated hologram of the mirror is tested by the null lens. The hologram, which is only 40 mm in diameter for a 3.5-m $f/1.75$ primary mirror, is made so it will appear as if it were a perfect primary mirror to the null corrector. The test is easy to perform to high accuracy for several reasons: it is a null test, it is insensitive to alignment errors, and no optics other than the hologram are required. The hologram is designed and fabricated independently from the null corrector, so agreement between the two indicates a high probability that both are correct.

The hologram is simply a circular grating or reflective zone plate on a flat substrate. The holograms used at Steward Observatory are made by etching concentric grooves into fused silica substrates and coating with reflective aluminum. The CGH patterns are fabricated by replicating masks written using electron beam lithography. The spacing of the grooves is determined analytically to synthesize the shape of the wavefront that would be reflected by a perfect mirror. The groove depth and width are optimized to minimize fabrication costs while giving the correct 4% diffraction efficiency to yield high contrast fringes.

A layout of the CGH null test, shown in Fig. 1, depicts an Offner null lens[3,7] and CGH. No modifications are made to the null lens for performing this test; the null corrector tests the hologram in exactly the same manner used to test a primary mirror. The alignment of the test is surprisingly simple. The CGH is positioned at paraxial focus of the light from the null corrector. Once the CGH is near the correct position, the shape of the fringe pattern in the interferometer is used to align the hologram. Since the CGH appears to the null corrector as a complete primary mirror with the correct shape, the alignment of the hologram is exactly like that of the actual primary. The lateral translation, axial translation, and tilt of the null lens are adjusted to eliminate tilt, focus, and coma from the interferogram.

The holograms are designed to give about 4% diffraction efficiency into the desired order. This matches the intensity from the reference surface to give a high-contrast interference pattern. A pinhole positioned near the Shack cube rejects the stray orders of diffraction and lets only the desired order through. The size of the pinhole is optimized so that the area corresponding to the entire tested region of the mirror is free from spurious orders, but the spatial frequency cutoff is acceptable.

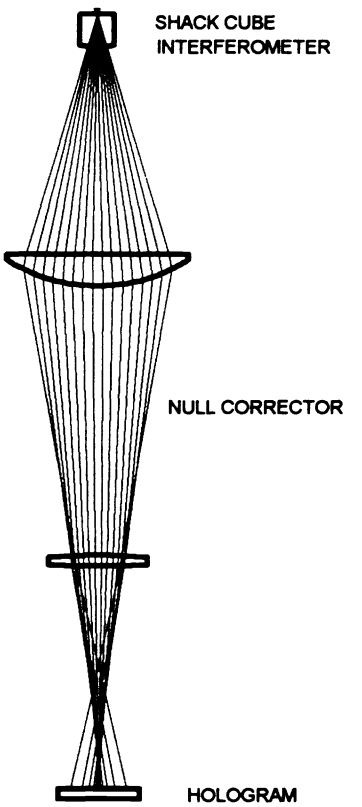

Figure 1. Layout of CGH test of null lens. The use of the CGH involves simply positioning the hologram at the correct location and making the measurement as if testing the mirror itself.

1.2. HOLOGRAM WAVEFRONT

The shape of the phase function created by the hologram (see Fig. 2) looks conical with little slope change over most of the CGH. This fortunate shape allows the CGH to work with no carrier at all. The radial slope in the wavefront itself is sufficient to act as a circular carrier with ring spacing nearly constant over most of the hologram. The CGH function shown in Fig. 2 shows why the conventional method of specifying CGH functions as a power series with even terms fails to converge for designing this hologram. There is a cusp at the center that is poorly modeled using a power series with a reasonable number of terms.

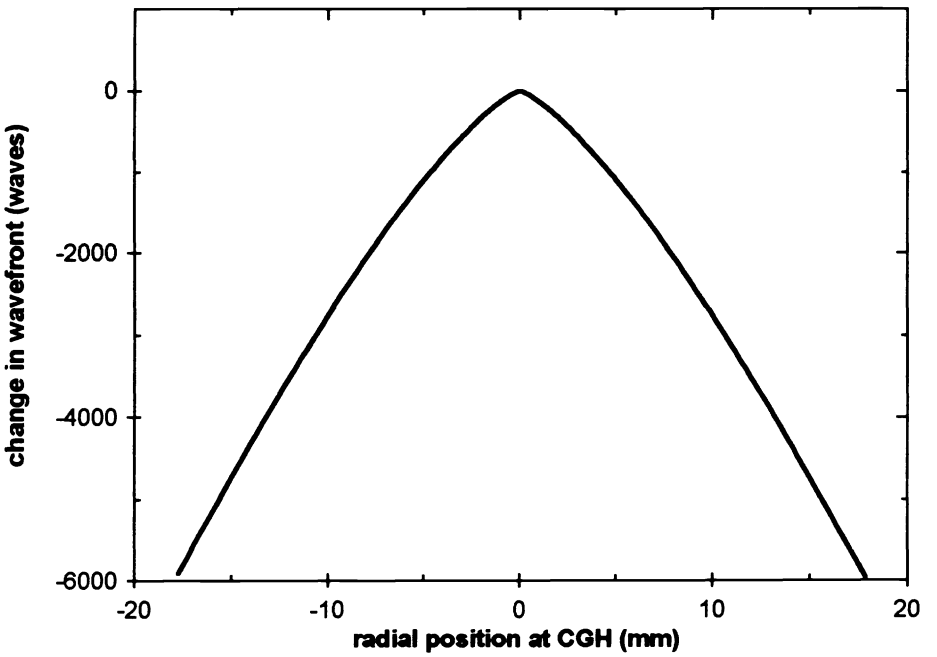

Figure 2. Wavefront phase function required of a paraxial-focus CGH to test a null corrector for a 3.5-m *f*/1.75 primary mirror. The conical shape allows the hologram to have nearly equally spaced rings.

2. CGH NULL LENS TESTS FOR TWO 3.5-m *f*/1.75 PRIMARY MIRRORS

The null correctors for two 3.5-m *f*/1.75 primary mirrors (for the ARC and WIYN telescopes) were successfully tested using computer-generated holograms. Both of these tests confirmed the null corrector conic constants within the test uncertainty of ±0.000078. The wavefront errors for the two null lenses were measured to be 0.022λ rms and 0.016λ rms at 632.8 nm. The surface measurements of the primary mirrors were corrected by subtracting these measured null lens errors from the data. The results of the null corrector measurements are shown in Table 1.

Since the ARC and WIYN telescope designs are quite different, the primary mirrors have different conic constants. Both 3.5-m primary mirrors had nominal focal ratios of *f*/1.75, but the ARC primary required a conic constant K of -1.0194 and radius of curvature R of 12280 mm and the WIYN required K = -1.0708 and R = 12250 mm. A null corrector was fabricated for testing the ARC primary mirror. After the completion of the ARC project, the null lens was altered to test the WIYN primary. The same lenses were used in both systems, but the spacings were changed.

Table 1. Summary of null lens measurements for two 3.5-m *f*/1.75 primary mirrors.

	ARC null lens	WIYN null lens
Conic constant of null lens measured with CGH	-1.01927 ± 0.00008	-1.07077 ± 0.00008
Expected conic constant from null lens analysis	-1.01933 ± 0.00008	-1.07079 ± 0.00008
Wavefront measured using CGH (at 632.8 nm)	0.022λ rms	0.016λ rms
Expected wavefront from null lens tolerance analysis	0.046λ rms	0.046λ rms

2.1. TEST DESCRIPTION

The null correctors were tested using computer-generated holograms as described above. The holograms were fabricated using electron beam lithography. The actual holograms were contact printed from master patterns that were made on an electron beam writer. A complete description of the process for making the holograms is given elsewhere[3].

Each null corrector was tested by placing the appropriate hologram at the paraxial focus of the light from the null lens. This was easily accomplished since the paraxial focus occurs at the end of the caustic where the light forms a bright spot. The CGH was translated laterally until this spot was centered on the hologram, and it was moved vertically to minimize the size of the spot. These coarse adjustments were used to get the CGH aligned closely enough that the fringe pattern was visible. The CGH was then translated laterally, axially, and gimbaled about horizontal axes to null the fringes of tilt, focus, and coma.

The holograms were measured using phase shifting interferometry, using exactly the same procedures as the primary mirror measurements. The interference patterns had uniform, high contrast. An interferogram from the test of the ARC null lens is given in Fig. 3. The spurious orders of diffraction were adequately blocked by a 200-μm pinhole. A bright spot from the -1 diffracted order is visible inside of the central hole in Fig. 3. The imaging systems were unaltered between the primary mirror testing and the CGH testing to allow direct comparison between the measurements. Because the imaging optics were designed to form an image of the primary mirror onto the detector array and the CGH was located near the center of curvature of the mirror, the hologram could not be focused onto the CCD. This fact requires the hologram to be oversized to keep edge diffraction from affecting the measurement.

Figure 3. Interferogram of computer-generated hologram through the ARC null lens. This single interferogram shows speckle, non-uniform illumination, air motion, and coma due to misalignment.

The azimuthal errors in the holograms were removed from the null lens measurements by averaging many data maps taken with the CGH at different rotational positions. When an average of 15 maps is taken with the CGH at equally spaced rotational positions, the non-axisymmetric errors in the CGH with terms through $\cos(14\theta)$ order average out while the errors in the null lens remain. It was easy to make many measurements with the CGH because the short path length reduces vibration and seeing, allowing rapid collection of data with minimal noise.

2.2. HIGH-FREQUENCY HOLOGRAM ERRORS

The encoding, digitizing, and writing of the holograms cause significant high-frequency errors in the diffracted wavefront. The hologram rings were encoded as chains of polygons that approximate the desired circles. Over many rings this approximation is excellent. However, the presence of the polygon vertices and high-frequency errors in the e-beam writing cause relatively large wavefront errors over short distances.

A phase map of a single holographic measurement of the ARC null lens is shown in Fig. 4. High-frequency features, as well as some low-frequency variation, are apparent in this figure. The cross pattern is an artifact of the symmetry used in encoding the pattern.

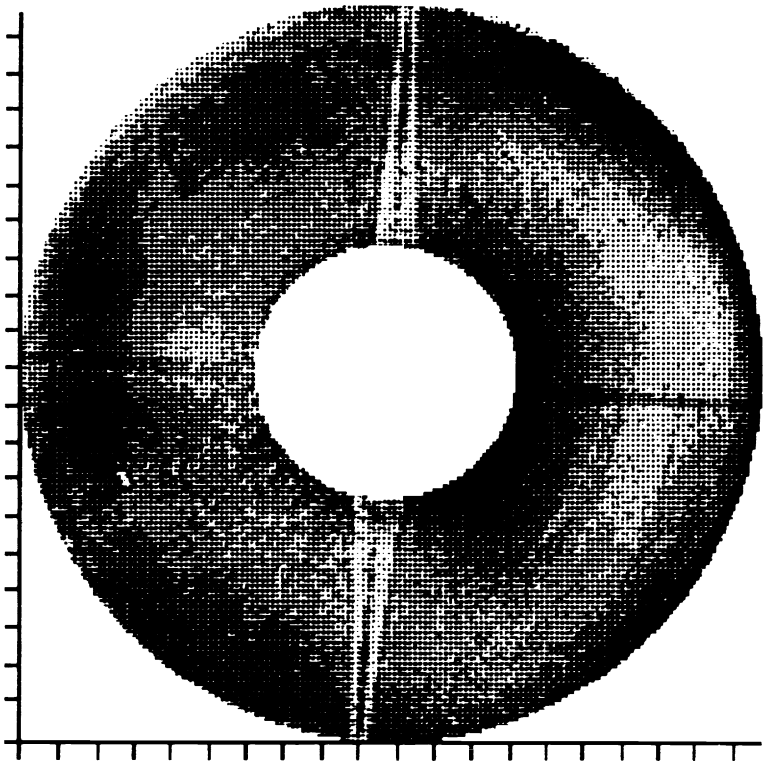

Figure 4. Phase map of a single CGH measurement showing high-frequency hologram errors. This map shows the surface errors (half of the wavefront errors) when testing the ARC null lens with a CGH. The map consists of contours at 10 nm intervals, showing variations from -40 to 40 nm. The total surface variation is 11.2 nm rms. The discontinuous contours show the high-frequency hologram errors.

The effect of the high-frequency structure is greatly reduced by taking an average of many measurements with the hologram rotated to different orientations. To further filter out the high-frequency errors from the hologram, a 36-term Zernike polynomial fit was made to the data. The null lens errors were then represented using the polynomial fit. This fit also filters out any high-frequency errors in the null lens. However, the null lens errors, which originate from misalignment, surface figures, and glass inhomogeneity, will have a negligible high-frequency component[3].

2.3. CORRECTIONS TO THE DATA

Corrections to the data were required for the CGH test of both the ARC and the WIYN null correctors. The hologram measurements had several known errors that were quantified and subtracted from the data. These errors were due to small differences in wavelength, radius of curvature, and conic constant between those assumed for the design of the holograms and the final values. The correction terms that were subtracted from the data were remapped according to the measured mapping distortion in the null lens. A detailed description of the calculation for these error terms is given elsewhere[3,4].

2.4. RESULTS OF NULL LENS TESTS

The ARC and WIYN null lenses were measured at 11 and 15 equally spaced rotational positions. The corrections made to the ARC data correspond to -1.5 nm P-V spherical aberration. The WIYN data required a larger correction of 57 nm spherical aberration because of a 3.5 mm difference in the radius of curvature assumed for the fabrication of the CGH and the final value used for the null corrector. These corrections were remapped to include the imaging distortion in the null correctors. After making these corrections, the CGH measurement of the ARC null lens found -11.4 nm spherical aberration corresponding to a conic constant error of -72 ppm. The measured spherical aberration in the WIYN null corrector was only -3 nm, corresponding to a conic constant error of -19 ppm.

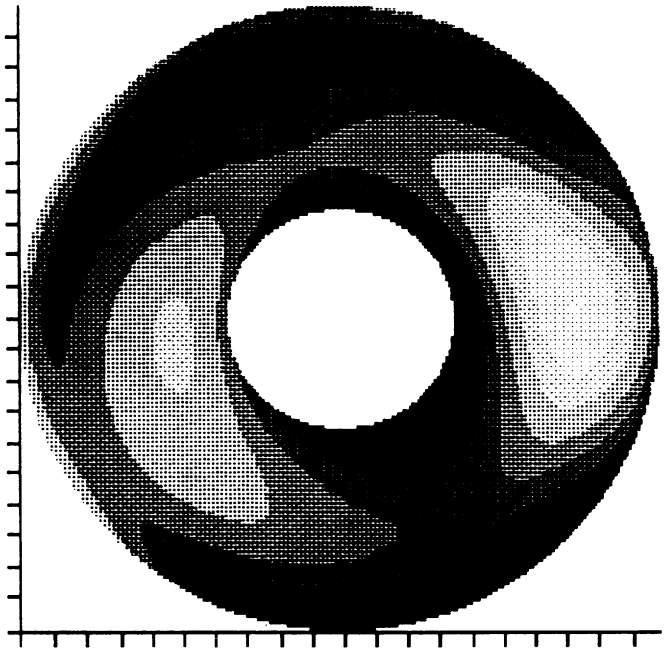

Figure 5. Contour map showing measured null lens error of 7.6 nm rms for ARC primary mirror as represented by a 36-term Zernike polynomial fit. Surface contours are plotted at 5 nm intervals over a range from -20 nm to 20 nm.

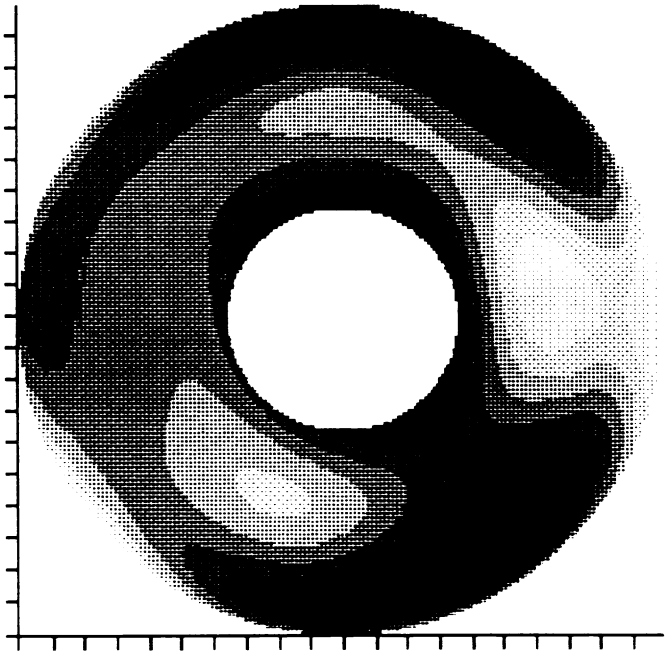

Figure 6. Contour map showing measured null lens error of 5.1 nm rms for WIYN primary mirror. The surface errors, computed from a 36-term Zernike fit to the data, are plotted with contours at 3 nm intervals over a range from -12 nm to 12 nm.

A visual comparison between measurements of the ARC null lens (Fig. 5) and the WIYN null lens (Fig. 6) shows a strong correlation. This is expected because the largest source of error in the null lenses, the refractive index inhomogeneity, is the same for both systems. The alignment errors are expected to be different.

2.5. ERROR ANALYSIS

The error terms originate from three sources: the CGH itself, the implementation of the test, and the analysis of the data. These errors were analyzed for the null correctors for the 3.5-m *f*/1.75 primaries, taking the worst case for each term. Only spherical aberration was considered because it is the most likely null corrector error[1,2,3] and the azimuthal errors are removed by rotating the hologram.

The errors in the hologram come from the surface figure, groove pattern distortion, and etch depth variations. The 50-mm substrates were specified to be flat to $\lambda/20$ P-V. The surface figure error that causes pure third-order spherical aberration (fourth-order dependence on r) in the null lens test has the cone-shaped appearance in Fig. 2. For the error analysis, it was assumed that this component of the figure error is less than $\lambda/20$. The e-beam writer has errors as large as ± 0.15 μm and printing errors can be as large as ± 0.2 μm. The encoding and digitization errors are not considered because they cause high-frequency errors that do not affect the conic constant. The grooves were specified to be etched to a depth of $\lambda/4$ with less than 5% depth variation over the entire aperture. The error analysis assumes the worst case of 5% depth variation causing pure spherical aberration. The gross errors discussed below are not included here because they cause phase discontinuities that are easily recognizable.

The uncertainty in the laser wavelength has several components. The uncertainty in the laser frequency is determined by the width of the Doppler-broadened gain of the neon transition. The frequency of a single-mode, unstabilized HeNe laser will be 473612 ± 1 GHz[8]. Errors in the refractive index of air caused by errors in the temperature and pressure measurements will cause an error in the wavelength. The thermal expansion of the fused silica holograms will also cause measurement errors proportional to the temperature difference between fabrication and use of the CGH.

The errors in data analysis are due to the uncertainty of the Zernike polynomial fit to the data and the uncertainty of the mapping between the mirror and the image. The Zernike polynomial fit of spherical aberration is estimated to be uncertain to $\pm 0.003\lambda$. An error in the distortion coefficient of 0.5% would cause an error of 0.0001λ in the 0.06λ spherical aberration correction to the WIYN data. A 1% error in the definition of the edge, corresponding to 1 pixel, would cause an additional 0.0024λ error.

These errors are summarized in Table 2 in terms of the uncertainty in the Zernike spherical aberration coefficient $Z8$ and the conic constant dK. The estimated uncertainty of the test is found by taking a root-sum-square (RSS) of the independent terms.

Table 2. Error budget for CGH test of null correctors for 3.5-m $f/1.75$ primary mirrors.

Error term	Value ± uncertainty	±Z8 (waves)	SDK (ppm)
Manufacturing errors			
write errors	0.15 μm over 20 mm radius	0.0054	32
print errors	0.2 μm over 20 mm radius	0.0072	43
substrate flatness	$\lambda/20$	0.0083	50
etch depth variations	5% of $\lambda/4$	0.0010	6
Errors in use			
CGH temperature	21 ± 3° C	0.0014	8
laser frequency	473612 ± 1 GHz	0.0011	6
air pressure	697 ± 5 mm Hg	0.0010	6
air temperature	21 ± 2° C	0.0011	6
Data analysis error			
mapping distortion error	6.7 ± 0.5 %	0.0001	1
edge definition error	1 pixel	0.0024	14
fit error $\Delta Z8$		0.0030	18
RSS		**0.0131**	**78**

The measurements of null corrector conic constants for the ARC and the WIYN primary mirrors are estimated to have a 78 ppm uncertainty. Additional uncertainty in determining the conic constant of the primary mirrors is caused by the uncertainties in the measured radii of curvature and in the measurements of the primary mirrors through the null corrector. The net uncertainty of 100 ppm in conic constant for each primary mirror is well within the telescope specifications.

3. MEASUREMENT OF NULL LENS WITH A KNOWN ERROR

To verify the CGH null lens measurement technique, the null lens for the ARC primary mirror was remeasured after making a deliberate spacing error of 90 μm. The spherical aberration that was measured using the CGH test closely matched the amount predicted by a computer simulation. This test confirmed the ability of the CGH null lens test to accurately quantify the null lens error.

After the CGH test of the ARC null lens was completed, a deliberate error was introduced into the null corrector. The large relay element on the null corrector was shifted 90 ± 5 μm towards the Shack cube, and the runout of the element was nulled to ± 3 μm. The CGH was used to measure the respaced null lens. The wavefront was shown to have 0.453λ P-V spherical aberration, corresponding to an effective error in the conic constant of 0.00091.

A computer simulation of the test of an ideal primary mirror with this perturbed null lens predicted a wavefront with 0.51λ P-V spherical aberration. Coefficients for third- and fifth-order spherical Zernike polynomials were fit and used to represent this wavefront. The expected wavefront was calculated by adding the Zernike terms to the measured error in the null lens shown in Section 2. This resulted in a wavefront with 0.477λ P-V spherical aberration -- in excellent agreement with the actual measured value.

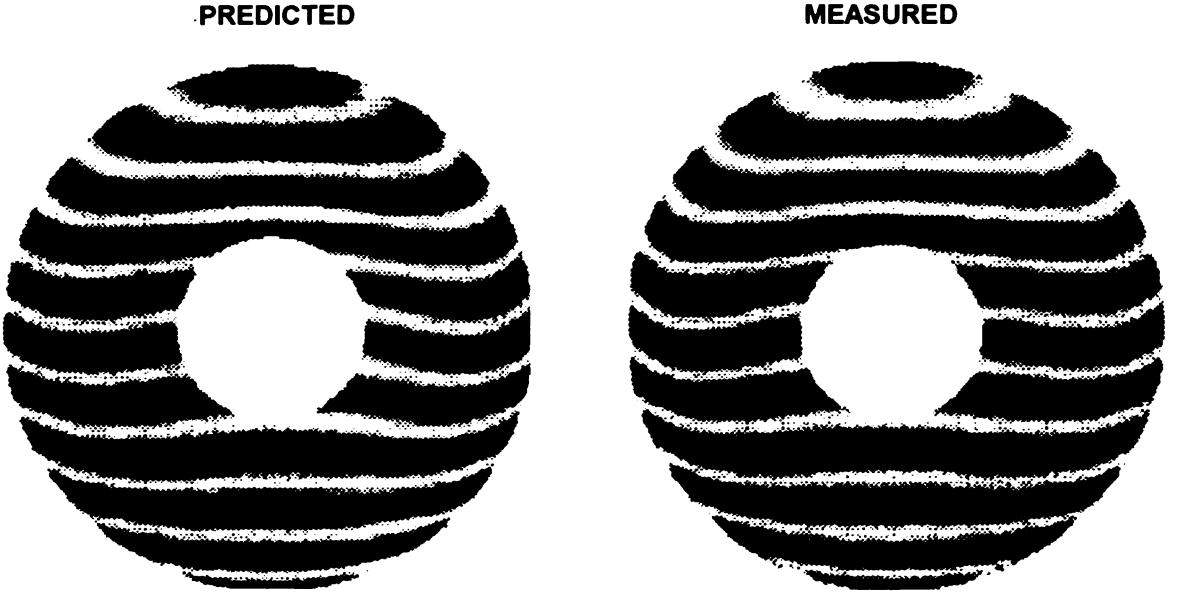

Figure 7. Comparison showing the excellent agreement between the predicted and actual measured effect of intentionally inducing a 90 μm spacing change in the ARC null lens. These interference patterns, calculated from the measured phase variations and those predicted by the simulation, are different by 0.01 λ rms.

4. VERIFICATION WITH A CGH REPRESENTING A SPHERICAL MIRROR

Reference holograms were fabricated to allow direct verification of the fabrication accuracy. The reference holograms simulated spherical *f*/1.75 mirrors in order to closely match the geometry of the above holograms, but to allow accurate testing with a Fizeau interferometer. The two null lens holograms and the first reference sphere CGH were fabricated at the same time using identical techniques. The two null lens holograms were highly accurate, as indicated by the excellent agreement between the holograms and the null correctors, but the reference CGH had a gross error. This error caused a step in the diffracted wavefront near the edge of the part. Six more reference holograms printed from the same master did not have this error. The reprinted holograms had only small errors consistent with the error analysis in Table 2. Three holograms for a test of another null lens, described in the next section, also had gross errors of the same form.

4.1. TEST DESCRIPTION

The reference holograms simulated 40 mm diameter convex or concave spherical surfaces with 134.4 mm radii of curvature. The holograms were tested both as concave and as convex spheres using a Fizeau interferometer (See Fig. 8). It is useful to test the CGH at both sides of focus to allow the separation of the flatness errors from the errors in the groove pattern. On either side of focus, variations in surface figure cause the same wavefront error -- a bump is a bump, although the image of the optic rotates 180°. Since the sign of the diffracted wavefront changes when the test is changed from convex to concave, the wavefront errors due to the hologram groove pattern distortion also change sign. This allows the separation of the hologram groove errors from flatness errors. To calculate the flatness errors, the results of the two measurements are averaged (after a 180° rotation), and the diffraction errors cancel. The diffraction errors are equal to half the difference of the convex and

concave measurements. Taking this difference, flatness errors in the hologram and reference surface errors with even symmetry cancel out.

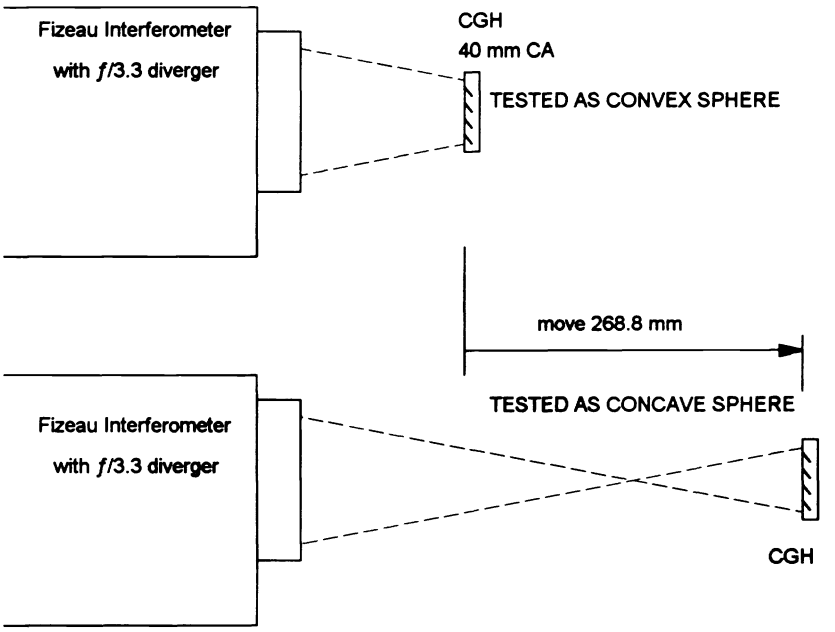

Figure 8. Fizeau test of CGH as both convex and concave spheres. Apart from a 180° image rotation, phase errors due to surface figure are identical for both cases and phase errors due to ruling distortion have opposite signs.

This test is insensitive to scale error in the hologram. Scale error in the CGH for the null lens test causes spherical aberration, but a scale error in the sphere hologram causes only power. Without the ability to measure the radius of curvature of the hologram accurately, it is impossible to determine whether or not the CGH has the correct power from the diffracted wavefront. The scale of the holograms was determined independently by measuring the positions of fiducial marks.

4.2. RESULTS FOR A FLAWED HOLOGRAM

The first spherical hologram had a gross printing error shown in Fig. 9. A sharp step occurred at a narrow zone near the edge of the CGH. The error was definitely not axisymmetric: the zonal step was off center by several mm and the phase error was larger on one side than on the other. When the ring pattern was examined under a microscope, no discontinuities were apparent. Also, the substrate was measured to be flat to $\lambda/20$. Because of its sharp nature, the error was easily verified to be in the hologram and not in the measurement optics.

This phase step of half a fringe corresponds to a radial shift of the ring pattern of about 1 μm. This is a factor of 5 larger than what was expected from the process. The firm that printed this hologram did not have an explanation for the origin of this error. They did reprint the hologram from the same master. Although the source of the problem was not identified, the second part did not show the error. It was then assumed that the flaw was due to an unlikely problem in the printing. Unfortunately, this error has recurred during the fabrication of other holograms.

The null lens for a 3.5-m $f/1.5$ primary mirror was measured using three different computer-generated holograms. All three holograms had significant errors of the type described above causing steps in the phase. The errors were different for all three holograms and there were large regions in each hologram that did not have phase errors. The phase error precluded an accurate measurement of the null corrector, but based on all three holograms it was estimated that the null lens wavefront had less than $\lambda/5$ P-V spherical aberration.

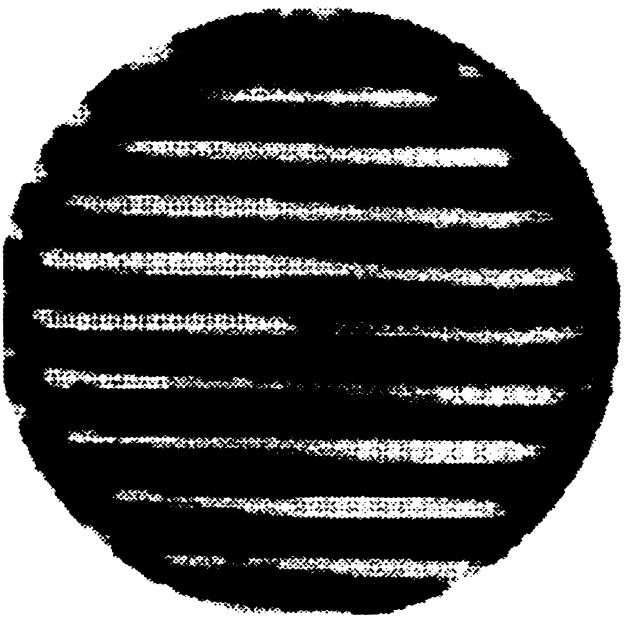

Figure 9. Interferogram from mis-printed CGH of a spherical reflector. A slightly offset step shows up at the outer edge.

Figure 10. Interferogram showing the measurements of a flawed hologram with the null corrector for a 3.5-m *f*/1.5 primary mirror.

Two important conclusions were drawn from the results of this test:

1. A fabrication error that causes a step in the phase can occur. The source of this error is not understood and this error may go undetected during fabrication.

2. If no such step error occurs, the accuracy of the holograms is described by the error analysis above.

The second point is weakly supported since it is based on such a limited number of holograms.

We are currently pursuing another fabrication process, defined in the next section, to manufacture holograms directly onto the final substrate. We are also researching methods of directly measuring the distortion of the final CGH, and may be able to certify the next holograms.

4.3. RESULTS FOR GOOD HOLOGRAMS

The reprinted reference CGH did not show the gross errors of the first, and is consistent with the assumed fabrication errors. This CGH was measured using a phase shifting Fizeau interferometer as both a convex and concave surface. By flipping and using the method described above, the optical surface was determined to deviate from flat by 3.2 nm rms and the hologram distortion caused errors of 7.6 nm rms. The diffraction error included 0.016λ P-V spherical aberration, which corresponds to about 0.2 μm P-V hologram distortion. This is comparable to the expected spherical aberration for the null lens test given in Table 2.

Five more copies of the reference sphere were printed and tested to get an estimate of the statistics involved. None of these five had the discontinuous error described above. In fact, all five were nearly perfect. The usual high-frequency errors were present but very little spherical aberration showed up.

5. CONTINUING RESEARCH FOR HOLOGRAPHIC TESTING OF NULL CORRECTORS

The holographic null lens test is a powerful technique for confirming the accuracy of null correctors. Further work is required to solve the fabrication problems before making the holograms for testing the null correctors for the 6.5-m and 8-m mirrors. These holograms will be larger, thus more difficult and expensive, than those for the 3.5-m mirrors, so the cost of a flawed printing will be high.

5.1. DIRECT WRITING TO ELIMINATE PRINTING ERRORS

Since variations are found among holograms printed from the same master, an error in contact printing is likely to be the source of this problem. The holograms are fabricated by writing a master pattern onto a thin, chrome-coated photo mask with the e-beam writer. This pattern is transferred to the final thick substrate using contact printing. In contact printing, the master pattern is held in vacuum contact with the final substrate that has been coated with chrome and photoresist. Collimated ultraviolet light is projected through the master to expose areas defined by the gaps in the chrome pattern. After developing and etching, a chrome pattern remains that is the negative of the master.

The printing errors can be avoided by eliminating the printing step from the fabrication process. This may be done by writing the hologram onto its final substrate with the e-beam writer, so that no transfer of the pattern is required. Since the flatness of the hologram surface is critical, special substrates must be prepared that are flat to $\lambda/20$. The substrates must be coated, e-beam written, and etched. Unfortunately, the e-beam writers will only accept standard size substrates that are very thin and are difficult to polish to such precision. The standard 4-inch square substrate is only 0.090 inches thick so it will deflect according to its support forces.

To get around this problem, the thin substrates will be mounted onto a master flat that is thick enough to hold its figure when simply supported. The back surface of the hologram substrate will be held in vacuum contact with the reference surface of the flat. This is a common technique that opticians use for holding thin optics. The front surface of the substrate will then be polished to $\lambda/20$ as it is supported in this manner. When removed and placed back on to the master flat, in the same position with the same orientation, the figure of the top surface of the substrate should be repeatable. This can easily be verified to high accuracy.

The flat substrate will be removed from the flat, coated with chrome and resist, and written by the e-beam writer. When it is removed from the master flat, the figure will no longer be flat. This does not affect the fabrication of the CGH: the commercially available "ultra flat" substrates are only flat to 2 μm. It will be processed, etched, and coated to form the final hologram. It will then be mounted back onto the master flat, recreating the flatness of the substrate.

5.2. HOLOGRAM FOR A 6.5-m *f*/1.25 PRIMARY MIRROR

Assuming the fabrication problems are solved, the CGH null lens test is planned for all of the telescope projects at Steward Observatory. The computer-generated hologram for testing the 6.5-m *f*/1.25 has been designed. This hologram will be 136 mm in diameter and will consist of 10757 grooves. This is within the realm of existing lithographic technology, but it will be difficult and expensive to fabricate.

This hologram will be directly written on the final substrate that is 7 inches square and 0.25 inches thick. This substrate will be polished flat to $\lambda/10$ as it is supported on a master flat as described above. An error budget for this test, assuming much larger errors for the 136 mm CGH than for the 40 mm holograms, indicates a measurement accuracy of ±40 ppm for the conic constant[3]. The absolute accuracy of the wavefronts from the large holograms will not be as high as for the previous holograms. However, the ratio of the errors to the total surface asphericity, which determines the uncertainty in the conic constant, will be smaller.

A prototype of this hologram will be fabricated before the full CGH is made. This prototype, consisting of only a narrow diametrical slice across the circular hologram, will allow a test of the fabrication technique that requires only a small fraction of the cost of the full hologram. This diametrical slice will be useful for measuring spherical aberration in the null lens.

The CGH for testing the null corrector for the LBT 8.4-m $f/1.14$ primary mirrors will be 208 mm in diameter and require 17919 rings. This is beyond the current capability of current e-beam writers. Luckily, this CGH will not be required for several years, after which time the explosive growth of the electronic industry is likely to have spurred the development of larger and more accurate e-beam writers, or other fabrication alternatives.

6. CONCLUSION

The holographic test is a powerful new way of confirming the accuracy of null correctors. It was verified on two null correctors for highly aspheric mirrors, where the conic constants were measured to an accuracy of ±78 ppm. In addition, the measurement of a null lens with a known error showed excellent agreement with the predictions.

The holograms were fabricated from masters that were written using electron beam lithography. Large errors have occurred in the printing of the final holograms from the masters. These errors show up in the optical test as steps in the phase, but they are not evident during fabrication. The test of the conic constant of a third null corrector was limited to an accuracy of ±250 ppm by these errors. The source of these errors is unknown, so future holograms will be written directly onto the final substrate, requiring no printing.

Continued research is underway with the goal of providing an accurate test of the null corrector for the 6.5-m $f/1.25$ primary mirrors. This test is expected to measure the conic constant of the null corrector to an accuracy of ±40 ppm. This can be achieved using available e-beam writers and specially prepared substrates. The excellent results achieved in the first two null lens measurements have demonstrated the power and potential accuracy of this test. This test is planned for the verification of all future null correctors at the Steward Observatory Mirror Laboratory.

ACKNOWLEDGMENTS

This research was part of the author's Ph. D. dissertation in Optical Sciences at the University of Arizona under Prof. Roger Angel.

REFERENCES

1. L. Allen, J. R. P. Angel, J. D. Mongus, G. A. Rodney, R. R. Shannon, C. P. Spoelhof, "The Hubble Space Telescope optical systems failure report," NASA Report (NASA, Washington, D. C., November 1990).
2. R. N. Wilson, F. Franza, L. Noethe, and G. Andreoni, "Active optics IV. Set up and performance of the optics of the ESO New Technology Telescope (NTT) in the observatory," J. Mod. Optics **38**, 219-243 (1991).
3. J. H. Burge, *Advanced Techniques for Measuring Primary Mirrors for Astronomical Telescopes*, Ph. D. Dissertation, Optical Sciences, (University of Arizona, Tucson, 1993).
4. J. H. Burge, "A null test for null correctors: error analysis," in *Quality and Reliability for Optical Systems*, J. W. Bilbro and R. E. Parks, Editors, Proc. SPIE **1993**, in press (1993).
5. J. Espiard and B. Favre, "Contrôle en laboratoire de la qualité du système optique d'un télescope de 1,524 m de diamètre," *Nouvelle Rev. d'Optique Appliquée*, **1** (6), 395-400 (1970).
6. T. K. Korhonen, "Optics for the Nordic Optical Telescope," *Observational Astrophysics*, R. F. Nielson, ed., Proc. of "Nordisk Forskerkursus," (Copenhagen University Observatory, 1987) pp. 198-209.
7. A. Offner, "A null corrector for paraboloidal mirrors," Appl. Opt **2**, 153-155 (1963).
8. K. D. Mielenz, K. N. Nefflen, W. R. C. Rowley, D. C. Wilson, and E. Engelhard, "Reproducibility of helium-neon laser wavelengths at 633 nm," Appl. Opt. 7, 289-292 (1968).